Frontiers in Science and Engineering Volume 4 Issue 3, 2024
ISSN: 2710-0588

Multi-site Garbage Collection Robot based on Machine Vision

Hanxu Guo[1,*], Yifan Su[2], Saoye Bai[2], Tiehu Liu[2], Lijuan Zhu[2], Tongru Lin[2], Yukuan Sun[2]

[1] School of Mechanical Engineering, Tiangong University, Tianjin 300387, China

[2] School of Electronics and information Engineering, Tiangong University, Tianjin 300387, China

*Corresponding Author

Abstract

At present, the problem of garbage disposal has become an urgent problem to be solved in the global energy technology revolution and transformation and development. The mainstream garbage removal methods are manual picking and mechanical collection, which has low cleaning efficiency and high cleaning cost. In order to realize the convenient and efficient recycling and cleaning of land and water garbage, a new propeller dynamics model is proposed. Through the structural strength analysis and gas-liquid two-phase flow simulation analysis, combined with the aerodynamic theory, the propeller impeller model was optimized and its suitable working parameters were explored. Based on the paddle impeller mechanism, combined with the visual recognition and classification system controlled by the algorithm combining YOLO and template matching, a multi-site garbage recycling robot based on machine vision was designed, which realized the intelligent and multi-step integration of garbage recycling, and provided a new research idea for improving the way of garbage cleaning.

Keywords

Simulation Analysis; Garbage Disposal; Machine Vision.

1. Introduction

At present, garbage disposal has become an increasingly prominent environmental problem. How to effectively handle garbage and promote the development of circular economy has become the focus of current society. It is not only related to the environment, public health and resource utilization, but also related to global climate change and social civilization construction. closely related to sustainable development. The "Solid Waste Disposal Act" of the United States, the "Waste Disposal Act" of Japan, and the "Pollution Control Act" of the United Kingdom all point out the importance of garbage disposal and recycling. Our country's "Environmental Protection Law of the People's Republic of China" and "Environmental Sanitation Law of the People's Republic of China" also clearly set out the strategic tasks of protecting the environment, conserving resources and promoting the development of a circular economy. According to requirements, by the end of 2025, the utilization rate of urban waste resources must reach about 60%, and the garbage classification collection and transportation capacity should reach about 700,000 tons/day, basically meeting the needs of municipal domestic waste classification collection, transfer and disposal at or above the prefecture level. At present, domestic waste in my country is still basically disposed of in centralized piles or simple landfills. The environmental protection measures of the landfill seriously fail to meet the standards, and the landfill gas and leachate generated cause great pollution to the surrounding environment[1].

ISSN: 2710-0588

The multi-site garbage recycling robot proposed by the us based on machine vision has two main advantages:①A new amphibious paddle wheel mechanism was established and the mechanism's performance was verified. The feasibility makes it possible to use one machine with multiple functions in a land and water operation environment.② Adopt yolo v3 visual recognition classification algorithm, matched with the power navigation module to realize automatic cruising, salvage, A series of functions such as classification, cleaning of water surface and land surface garbage, and intelligent adjustment of cleaning tasks [2].

2. Paddle Impeller Mechanism for Multi-site Garbage Collection Robot Sub-section Headings

In order to meet the operating requirements of multiple working sites for the ship-shaped garbage recycling robot shown in Figure 1, we designed a new paddle wheel mechanism. The paddle wheel is a mechanism that generates propulsion force by rotating paddles in the water. It has webs on both sides and a paddle blade in the middle, which is fixed on both sides of the stern of the hull. As the driving device of the entire robot, we control the real-time output power of the motor to achieve differential speed and complete travel goals such as steering and U-turns. The overall material is magnesium alloy and its composite materials, a lightweight and high-strength metal material with a specific strength close to that of aluminum alloy, but with a lower density, which can reduce the overall weight and improve propulsion efficiency. The modeling of the paddle wheel mechanism is shown in Figure 2.

Figure 1. Overall modeling rendering of the garbage collection robot

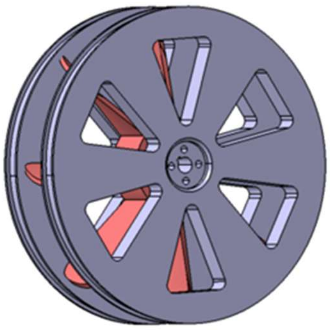

Figure 2. Modeling rendering of the paddle wheel mechanism

When the robot is working on the water surface, 60% of the lower part of the paddle wheel is immersed in the water. When performing garbage sorting and recycling work, the T60 motor drives the paddle wheel to rotate. The paddle blades cut into the water surface at a specific angle, producing a backward thrust on the water. At the same time, the water produces a reaction force on the paddle blades, pushing the hull forward. The blades are designed with a specific arc surface, which on the one hand reduces the impact of water entry, reduces stress

ISSN: 2710-0588

and makes the robot drive smoothly; on the other hand, it facilitates the outflow of water when the blades come out of the water, reducing unnecessary energy consumption. According to calculations, compared with the normal curved surface, we optimized the propeller's surface shape value and working parameters based on BP artificial neural network, effectively improving the efficiency by about 13.5%. Since the radial circle diameter of the paddle wheel blades is 250mm smaller than the radial circle diameter of the webs on both sides, which is 300mm, the outer webs support the robot on the ground. When the robot is working on land, the paddle wheels are driven by the T60 motor to advance at a speed of 0.3m/s, while ensuring the completion and efficiency of garbage cleaning.

The outer rings of the webs on both sides are covered with polyurethane rubber (PUR) tires. Polyurethane rubber is a polymer material with excellent wear resistance and elasticity. It is suitable for manufacturing the tire soles and sidewalls, effectively improving the tire's wear resistance, fatigue resistance and road grip performance.

Considering the overall structural strength, during actual navigation, there is a difference in buoyancy between the left and right sides of the hull. As a result, larger shear stress and moment are generated in the connection area between the left and right rear wheels. Because this robot needs to complete the work of garbage classification and collection, the hull is wider, and the paddle wheels need to rotate at differential speeds when turning, which has a greater stress moment than ordinary ships. In order to reduce the risk of the hull deforming and disintegrating under working water conditions, this ship-type robot must be designed with a more load-bearing structure. Only connecting it through the main frame is far from meeting the standards of structural mechanics. We enhanced the overall strength and stiffness by adding high-strength fibers and increased wear resistance. Use high modulus glass fiber and YT-CC302Q two-component epoxy resin glue in some vulnerable parts (such as the stress contact surface of the bearing end cover connecting the blade and the web and the connecting shaft of the two blade impellers) Mix and pressurize for 8 hours in a near-vacuum environment to produce some composite connectors. The durability of vulnerable parts can be increased by up to 30%[3]to achieve the guarantee The purpose of reducing the weight of the hull as much as possible while improving the strength of key parts is to extend the service life of the paddle wheel mechanism itself.

2.1. Determination of Blade Surface

The blade design based on the coordinate transformation equation of the propeller surface type value is currently a widely used method for determining propeller parameters. The geometric view combined with the traditional propeller drawing method can be expressed vividly and accurately. The geometric view of the traditional propeller drawing method requires the drawing of orthogonal projection, side projection, and extended contour drawing of the propeller blade to ensure that the structure and shape of the propeller can be fully expressed[4]. Based on data such as the blade profile size table and blade cross-section size table provided by the propeller, the main view shows the front projection of the propeller, showing the shape and size of the propeller, as well as the position of the blades relative to the axis. The top view shows the top projection of the propeller, showing the distribution of the blades and their position relative to the shaft. The left view shows a side projection of the propeller, showing the shape and size of the propeller, as well as the overall structure of the propeller.

As shown in Figure 3, based on the baseline OH, two key angle parameters are introduced, θ represents the longitudinal oblique angle, and ϕ represents the pitch angle, to describe the positioning and properties of the propeller in more detail. In the global coordinate system OXYZ, the intersection point of the plane OXY parallel to the hub end face and the baseline OH is defined as O', and the entire coordinate system OXYZ is parallel to the $O'X'Y'Z'$ coordinate system. By rotating the $O'X1Y1Z1$ coordinate system to coincide with the $O'X'Y'Z'$ coordinate

ISSN: 2710-0588

system, the coordinate system transformation is simplified, providing a better framework for propeller modeling and analysis and helping to solve complex problems related to propeller motion and performance. Question:

$$\begin{bmatrix} X_1 \\ Y_1 \\ Z_1 \end{bmatrix} = \begin{bmatrix} 1 & 0 & 0 \\ 0 & \cos\varphi & \sin\varphi \\ 0 & -\sin\varphi & \cos\varphi \end{bmatrix} = \begin{bmatrix} X' \\ Y' \\ Z' \end{bmatrix}$$
$$\begin{bmatrix} X' \\ Y' \\ Z' \end{bmatrix} = \begin{bmatrix} 1 & 0 & 0 \\ 0 & \cos\varphi & -\sin\varphi \\ 0 & \sin\varphi & -\cos\varphi \end{bmatrix} = \begin{bmatrix} X_1 \\ Y_1 \\ Z_1 \end{bmatrix}$$
$$\begin{bmatrix} X \\ Y \\ Z \end{bmatrix} = \begin{bmatrix} X' + R_i \cos\Psi' \\ Y' \\ Z' - R_i \tan\theta \end{bmatrix} \tag{1}$$
$$\Psi' = Y'/R$$
$$\begin{bmatrix} X \\ Y \\ Z \end{bmatrix} = \begin{bmatrix} R_i \cos\dfrac{Y_1\cos\varphi - Z_1\sin\varphi}{R_i} \\ R_i \sin\dfrac{Y_1\cos\varphi - Z_1\sin\varphi}{R_i} \\ Y_1\sin\varphi + Z_1\cos\varphi - R_i\tan\theta \end{bmatrix}$$

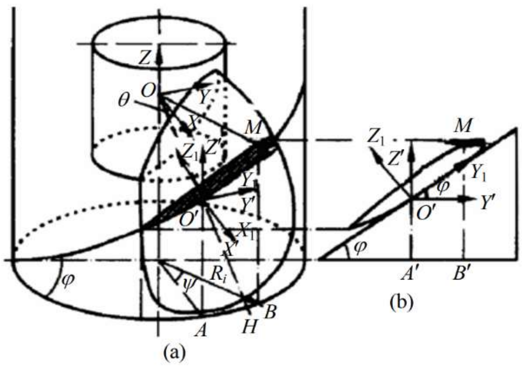

Figure 3. Schematic diagram of coordinate transformation

Based on the propeller surface type value determined by the coordinate transformation equation, combined with the propeller parameters of robot work and current industrial production, we preliminarily determined the parameters of the propeller impeller blades as shown in Table 1:

Table 1. Paddle Wheel Blade Parameters

parameter	data	parameter	data
number	8	Blade width	80mm
diameter	205mm	Minimum root thickness	3.5mm
Disk ratio	0.55	pitch ratio	1.6
apical twist	13.8°	hub diameter ratio	0.18
root width	6.27mm	Center section normal angle	24.25°

ISSN: 2710-0588

2.2. Paddle Wheel Simulation Analysis based on Ansys and Fluent Surface

The paddle wheel is an important part of the robot. It is responsible for the power output of the entire robot. It is required to bear various reaction forces and loads on the bearing surface at the same time. It is also the main component and important bearing component and force transmission that needs to withstand the turning moment of the robot and is also subject to pressure. part. Since the nature of the load is dynamic, it is necessary to pair the simulation and analysis of the fluid-structure coupling characteristics of the robot with the structural mechanical performance to understand the decontamination status of the robot when it moves on the water at a certain speed, and to ensure that the hull is stressed and turned in all directions The structure is stable under torque and the stress and strain meet the requirements.

2.3. Grid Division and Determination of Simulation Starting Simulation Conditions

Taking into account the fact that the water flow is an ideal fluid, the rated output power of the T60 motor is constant, and the geometric periodicity of the propeller wheel, in order to save calculation time and improve calculation efficiency, only the one-way water flow channel where a single blade is located is used for calculations during the water surface test. Domains are analyzed[5]. The outer boundary is selected as the cylindrical flow area with a diameter of 1.5 times the thickness of the impeller as the wall boundary, the water velocity inlet is selected as the inflow boundary, and the pressure boundary is selected as the outflow boundary.

According to fluid dynamics, the flow conditions of the part connecting the blade and the intermediate shaft change greatly, and the part of the water in contact with the fluid has a greater viscosity. At this time, the flow is dominated by complex and disordered turbulent flow. The trajectories of fluid particles move irregularly in the turbulent flow, and they will produce random changes in different directions. [6] Therefore, when performing meshing, it is required to divide the connected parts more carefully. As shown in Figure 5, a hexagonal surface mesh with a length of 0.0025D is used in the area near the blade shaft connection, blade tip, and blade root, and a triangular surface mesh with a length of 0.005D is used in the remaining parts. A total of 483525 meshes are planned. The simulation results are in line with expectations[7].

Set the simulation starting conditions as: air pressure: 1.01×105Pa; ambient temperature: 310K; gravity acceleration: 9.81 m/s2; water flow (ideal fluid) speed 3m/s. Simulation area boundaries: water velocity inlet (inflow boundary), pressure boundary (outflow boundary) and wall boundary.

Figure 4. Grid division rendering

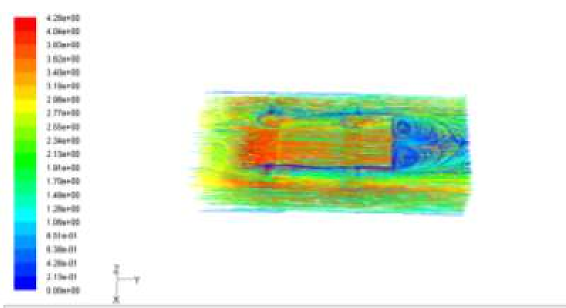

Figure 5. Fluent simulation rendering

2.4. Division Conclusion of Paddle Wheel Simulation Analysis

It can be seen from Figure 5 that when the paddle wheel model is in the test water flow, the webs on both sides of the paddle wheel are relatively smooth and flat, and there is no major change when the water flow passes by. Because the blades and web at the tail of the propeller wheel model cause sudden flow due to their rapid changes in shape, large vortices are formed at the bottom and tail of the wheel[8]. The existence of vortices directly leads to a sudden

ISSN: 2710-0588

decrease in pressure in this area, increasing the resistance of the hull when traveling on the water.

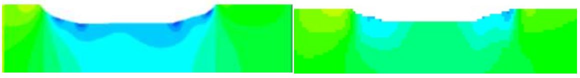

Figure 6. Pressure cloud diagrams in shallow water areas and deep water areas

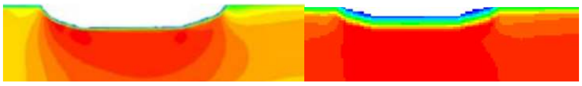

Figure 7. Pressure cloud diagrams in shallow water areas and deep water areas

During the physical experiment, we found that the depth at which the paddle wheel works greatly affects the overall propulsion efficiency. The draft of the paddle wheel is about 60% of its diameter. On this basis, the shallow water area and the deep water area are divided into shallow water areas and deep water areas by changing the vertical height of the bottom end of the paddle wheel model from the water bottom. The vertical height in shallow water area is 300mm and in deep water area is 1000mm. The pressure and velocity cloud diagrams of deep and shallow water areas are simulated on the fluent software, as shown in Figure 6 and 7.

By comparing with the experimental data, it can be seen that the simulation results can better simulate the resistance changes of the propeller impeller in the actual sailing state of the vehicle body under different sailing speeds and working environments, as well as the actual water flow field around the vehicle body.

When the robot sails in shallow water, the distance between the bottom of the paddle wheel and the water bottom is small. When the water flows through the bottom of the vehicle body, the flow rate under the vehicle is increased compared to the situation in the deep water area, and the backflow phenomenon increases. The viscous resistance is mainly determined by the flow field around the car body. The flow field changes in shallow water areas are reflected around the paddle wheel and concentrated at the bottom of the paddle wheel. At this time, the flow velocity at the bottom of the paddle wheel increases, and there is an obvious flow vortex at the bottom of the wheel, resulting in a sharp increase in viscous resistance. At the same time, the paddle wheel is affected by viscous resistance and water flow impact in the flow field, and the sailing position changes. Along with the mechanical vibration caused by the impact, the viscous resistance is further increased.

When the paddle wheel runs at high speed, an obvious vortex area is formed at the rear of the vehicle body, causing the instability of the water flow and a significant increase in negative pressure. When the impeller is operating at low speed, the water flow at the bottom and tail of the blade shows good flow direction stability, which confirms that research methods based on fluid dynamics simulation are useful in exploring such complex flow field problems. aspects of effectiveness.

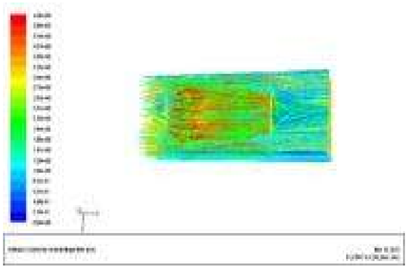

Figure 8. Optimized fluent simulation renderings

ISSN: 2710-0588

To sum up, the shape of the paddle wheel, sailing environment and sailing parameters have a great impact on reasonable and efficient sailing efficiency. Since wave resistance and air resistance have little impact on the experimental results, they will not be considered at the physical level for the time being. Combined with the test data, the viscous pressure resistance of the paddle wheel decreased by 28.6% from shallow water to deep water. From low-speed sailing to high-speed sailing, the heading efficiency has experienced a low-high-low change process. The highest point efficiency has increased by 21.9% compared to the original setting. This verifies the selection of a suitable sailing environment, appropriately increased amphibious vehicle speed and improved propeller wheel design. Feasibility of methods to achieve greater navigation efficiency. Finally, we streamlined the design of the area near the blade shaft connection, blade tip, and blade part, and made it clear that the working water depth should be greater than 800mm, and the sailing speed of 0.5-1m/s is the suitable working range. After optimization, it was divided according to the original grid and The conditions are set, and the effect is shown in Figure 8. It builds the basis of theoretical and experimental data for further research, and provides certain guidance for future design calculations and analysis.

3. Visual Recognition Classification Algorithm Combining YOLO

3.1. Advantages of YOLO V3

The YOLO v3 target detection algorithm is comprehensively improved by Redmon based on YOLO v2. Different from Darknet19 used by YOLO v2, YOLO v3 adopts a new network structure, as shown in Figure 9. The network structure of YOLO v3 contains a large number of 1×1 and 3×3 convolution layers, with a total of 53 convolutions. layer, hence the name Darknet53. Introducing the idea of residual learning, by adding a large number of residual blocks to the network, it effectively avoids the gradient explosion phenomenon caused by deepening the network layer model during the training process[9]. When using the softmax function for classification, when the target in the target border belongs to multiple categories, it can only be considered to be one category. YOLO v3 abandons the softmax function and uses multiple independent logistic regression classifiers to classify target objects. Each logistic regression classifier only determines whether the object in the target border belongs to the current label, that is, a simple binary classification, which realizes the definition of multiple classification labels for the same object.

	Type	Filters	Size	output
	Convolutional	32	3×3	256×256
	Convolutional	64	3×3/2	128×128
1×	Convolutional	32	1×1	
	Convolutional	64	3×3	
	Residual			128×128
	Convolutional	128	3×3/2	64×64
2×	Convolutional	64	1×1	
	Convolutional	128	3×3	
	Residual			64×64
	Convolutional	256	3×3/2	32×32
8×	Convolutional	128	1×1	
	Convolutional	126	3×3	
	Residual			32×32
	Convolutional	512	3×3/2	16×16
8×	Convolutional	256	1×1	
	Convolutional	512	3×3	
	Residual			16×16
	Convolutional	1 024	3×3/2	8×8
4×	Convolutional	512	1×1	
	Convolutional	1 024	3×3	
	Residual			8×8
	Avgpool		Global	
	Connected		1 000	
	Softmax			

Figure 9. YOLO v3 network structure diagram

ISSN: 2710-0588

3.2. Distance Determination

In order to solve the limitations of the traditional YOLO algorithm in object recognition and tracking, that is, it cannot directly identify the distance between objects and objects, this project has made an innovative attempt. We skillfully combine the traditional 2D YOLO algorithm with the monocular ranging algorithm to successfully realize real-time recognition and tracking of objects, and also accurately measure the distance between objects and robots. This breakthrough has greatly improved the positioning accuracy of robots in garbage collection tasks, making garbage picking more convenient and efficient.

The monocular ranging algorithm is designed based on the principle of pinhole model. It relies on known camera parameters, and through in-depth analysis of the images captured by the camera, it is possible to estimate the distance between the waste and the robot with relatively accurate accuracy. Through the perfect combination with the YOLO algorithm, we can not only accurately identify the presence of garbage, but also quickly determine the spatial distance between the garbage and the robot. The combination of this technology allows the robot to locate the garbage more accurately, greatly improving the success rate and efficiency of garbage collection.

$$D = \frac{F \times W}{P} \tag{2}$$

F is the focal length of the camera, W is the length or width of the object, and P is the width or length of the pixels occupied by the object in the camera. In the process of running YOLO for garbage identification and tracking, the robot can realize the distance measurement of garbage by collecting the above parameters.

3.3. Robot Travel Control based on PID Algorithm

In order to meet the needs of the robot to go to the garbage location smoothly and accurately for collection, we have introduced the classic PID algorithm in the control field. Combined with the advanced YOLO algorithm, the robot can accurately identify the garbage and extract the relative position of the garbage in the camera and the distance information between the robot and the garbage. Based on this information, the PID algorithm will precisely control the operation of the impeller to ensure that the robot can go straight and stable to the target location and successfully complete the garbage collection task.

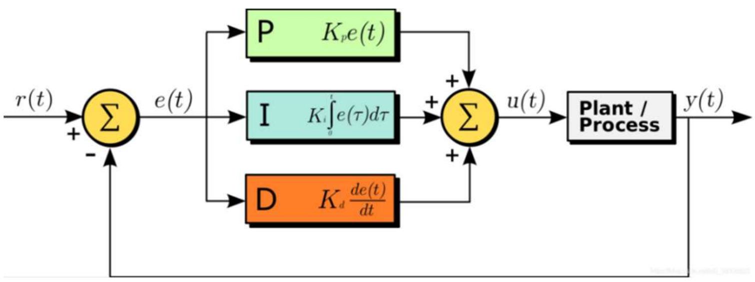

Figure 10. Block diagram of the PID algorithm

The PID algorithm is a common control algorithm that maintains stability. From the above block diagram, the relationship between e(t) and u(t) can be obtained:

$$u(t) = K_p e(t) + K_i \int_0^t e(\tau)d\tau + K_d \frac{de(t)}{dt} \tag{3}$$

ISSN: 2710-0588

The core of the PID control algorithm is to continuously calculate the error, in this project is to calculate the distance between the current position coordinates of the detected garbage and the target coordinate value, divide it into three steps to calculate a correction quantity, and act on the robot together with the three quantities. Through the flexible use of the PID algorithm, the robot can quickly and smoothly move in the direction of garbage and collect it.

3.4. Sample Database

Based on the tasks and working environment that the multi-site garbage recycling robot studied in this article needs to complete, a self-built computer vision data set was built. The data set contains real images of garbage that may appear on water and land in various scenarios. The training set contains a total of 22,004 images with annotations, and the test set contains a total of 5,626 images without annotations. The data set is divided into 8 categories: beverage bottles, packaging bags, batteries, small electronic equipment, fallen leaves, vegetable leaf peels, and miscellaneous items. The database label effect is shown in Figure 11. Responding to the national call for waste classification and taking the actual situation into consideration, the data set is reclassified into four categories of waste: the first two are combined into recyclable waste; batteries and small electronic equipment are combined into hazardous waste; vegetable leaf peels are kitchen waste; Miscellaneous is other garbage. The final number of samples in the training set was: 5231 recyclable waste, 5125 hazardous waste, 5525 kitchen waste, and 6123 other waste.

Figure 11. Recognition renderings

3.5. Real Machine Application

This research is dedicated to solving the complex challenges faced in the field of waste classification and robot operation, adopting a comprehensive technical solution to adapt to the changing real-world environment and the highly dynamic nature of waste targets. Among them, we mainly use the K210 embedded processor, a high-performance chip based on RISC-V architecture, with excellent computing power and energy efficiency.

Known for its low power consumption and high customizability, the K210 processor is particularly suitable for embedded computing and machine learning applications. It has a powerful neural network accelerator built-in, making it ideal for deep learning models. In our research, we make full use of the computing power of the K210 processor and regard it as a core component for garbage classification and robot visual perception. Combined with the YOLOV3 target detection algorithm, the K210 processor can efficiently identify garbage targets in real time, providing the robot with powerful perception and positioning capabilities. At the same time, the robot's motion control is taken care of by the MEGA2560 microcontroller to ensure that the robot can plan paths and perform tasks with high precision[10].

In addition, in terms of solving the problem of precise positioning of garbage objects, we adopt an innovative method to combine YOLO V3 target detection with template matching technology. When the robot's vision system captures a garbage object, we use the computing power of the

K210 processor to accurately measure the straight-line distance of the garbage object through monocular ranging technology, thereby achieving high-precision determination of the position of the garbage object. This ensures that the garbage object is always located in the center of the field of view, providing the robot with a high-precision operation and processing basis.

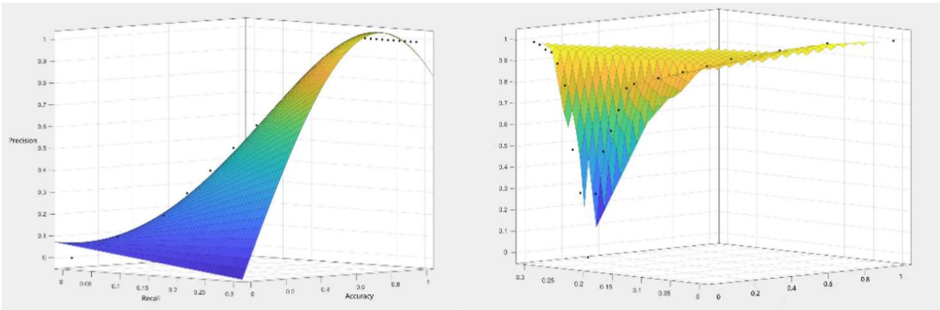

Figure 12. Iteration success rate

As can be seen from the figure, as the number of iterations increases, the stable values of Precision and Recall of the migration learning model for garbage recognition are used as the correct indicators to judge the recognition effect. From the beginning of training to the mAP (general term for Precision and Recall) value tends to The time it takes to stabilize is used as the training time. The performance comparison results of model are shown in Figure 12.

In this comprehensive technical solution, we also introduced monocular ranging technology to further enhance the accuracy of garbage classification and robot operation. Monocular ranging is a method of measuring the distance between an object and a camera by analyzing images acquired by a single vision sensor. This technique typically uses information such as the size, shape, and parallax of objects in an image to estimate the distance from the object to the camera. Monocular ranging technology is used to accurately locate garbage objects to ensure that they are always located in the center of the field of view, thereby supporting high-precision operation and processing of the robot.

4. Conclusion

This paper comprehensively uses BP artificial neural network optimization, Fluent simulation analysis, YOLO V3 target detection algorithm and monocular ranging technology to fully utilize the potential of modern computer vision and deep learning technology, demonstrating an optimized propeller propulsion rate optimization and comprehensive The method of solving complex garbage classification has laid a solid foundation for the research and development of multi-site garbage recycling robots. This comprehensive solution has broad application prospects in the fields of waste management, environmental protection and sustainable development, and is in line with the current technological development trends of intelligence, automation and sustainability. At the same time, this research also incorporates the current scientific and technological development trends, emphasizing the importance of simulation, artificial intelligence, optimized design, environmental protection and sustainable development, and provides a powerful academic example for future technology research and application. In the future, this technology is expected to further promote the development of intelligent robots and garbage classification technology, providing innovative solutions to complex real-world problems.

ISSN: 2710-0588

Acknowledgments

Supported by National Undergraduate Training Program for Innovation and Entrepreneurship (No.202310058008).

References

[1] Mert G ,Wuhuan Z ,Nimna M , et al. Survey on the Current Leachate Treatments of Public Municipal Solid Waste Landfills and the Potential Impact of Per- and Polyfluorinatedalkyl Substances in the Eastern and Northwestern United States. [J]. Journal of the Air & Waste Management Association (1995), 2023, 73 (8): 638-648.

[2] Anandakumar H ,Babitha R L ,Suriya M , et al. An improved single short detection method for smart vision-based water garbage cleaning robot [J]. Cognitive Robotics, 2024, 4 19-29.

[3] Kleven M J G ,Sverre S ,Magnus O F . An Efficient Method for Design and Powering Prediction of Fast Slender Catamarans [J]. Ocean Engineering, 2023, 286 (P1).

[4] Robotics; Study Results from Discipline of Mechanical Engineering Provide New Insights into Robotics (Conceptual Design of a Hybrid Propulsion Underwater Robotic Vehicle With Different Propulsion Systems for Ocean Observations) [J]. Robotics & Machine Learning, 2019.

[5] Qingping L ,Ming L ,Yao Z . Application of QGA-BP Neural Network in Debt Risk Assessment of Government Platforms [J]. International Journal of Information Technology and Web Engineering (IJITWE), 2023, 19 (1): 1-18.

[6] Zhu L . Network security threat detection technology based on EPSO-BP algorithm [J]. EURASIP Journal on Information Security, 2024, 2024 (1).

[7] Nourmohammadi H ,Keighobadi J ,Bahrami M . Design, dynamic modelling and control of a bio-inspired helical swimming microrobot with three-dimensional manoeuvring [J]. Transactions of the Institute of Measurement and Control, 2017, 39 (7): 1037-1046.

[8] Karabulut C U , Özdemir H Y ,Barlas B . Numerical Investigation of the Effect of Surface Roughness on the Viscous Resistance Components of Surface Ships [J]. Journal of Marine Science and Application, 2022,21(03):71-82.

[9] Weijia D ,Lingyan P ,Qi Z , et al. Athlete target detection method in dynamic scenario based on nonlinear filtering and YOLOv5 [J]. Alexandria Engineering Journal, 2023, 82 208-217.

[10] Zijun Z ,Xiang F ,Huiqun Y , et al. Cooperative density-aware representation learning for feShaobo M ,Hantao Y ,Hongtao X , et al. Multi-Objective Matrix Normalization for Fine-grained.

[11] Visual Recognition. [J]. IEEE transactions on image processing : a publication of the IEEE Signal Processing Society, 2020, 29 4996-5009.w-shot visual recognition [J]. Neurocomputing, 2022, 471 208-218.